Mixed Reality Visualization and Interactive Hemodynamic Computation of the Human Brain

Fenfen Qi
Department of Mathematics
University of Macau
Macau, China

Yingzhi Liu
Department of Mathematics
University of Macau
Macau, China

Yujie Gong
Department of Mathematics
University of Macau
Macau, China

Jing-Yuan Wang
Department of Mathematics
University of Macau
Macau, China

Jie Zhou
Department of Mathematics
University of Macau
Macau, China

Rongliang Chen
Shenzhen Institute of Advanced Technology
Chinese Academy of Sciences
Shenzhen, Guangdong, China

Ruey-Song Huang
Center for Cognitive and Brain Sciences
University of Macau
Macau, China

Xinhong Wang
Department of Radiology
The Second Affiliated Hospital
Zhejiang University School of Medicine
Hangzhou, Zhejiang, China

Li Luo
Department of Mathematics
University of Macau
Macau, China

Xiao-Chuan Cai
Department of Mathematics
University of Macau
Macau, China

***Abstract*—We develop a mixed reality platform to visualize some of the anatomical structures and functional areas of the human brain and interactively compute the blood flows in the cerebral artery with a special focus on the impact of aneurysms. The geometrical details and the cerebral artery are segmented from MRI images, and the functional areas of the brain are identified and mapped by a functional brain atlas. The platform consists of a holographic device with camera to capture the physical object and also hand gestures from the user to operate on the digital object, and a GPU-based platform manager to fuse the data from the holographic device and the computing system. Another major component of the platform is a parallel computer connected to the platform manager for the near real time computation of the hemodynamics of the cerebral flows using a highly scalable domain decomposition algorithm. Such a platform has potentially many applications in brain sciences, and in this paper, we focus on its application in the visualization of the digital brain including the area, volume and thickness of certain functional areas, the risk assessment of rupture and the surgical planning for cerebral aneurysms.**

***Index Terms*—Mixed reality visualization, human brain, functional atlas, hemodynamics, unsteady incompressible Navier-Stokes equations, interactive parallel computation**

I. Introduction

The human brain is a complex and crucial organ responsible for receiving, storing, processing information and regulating various activities of the body. Interactive 3D visualization of the brain is increasingly used by scientists and surgeons to accurately target the region of interest to understand the functionalities of a certain area. Using imaging technologies such as computed tomography (CT) or magnetic resonance imaging (MRI), clinicians study the brain from a series of 2D slices that provide a lower level of realism than a full 3D image. With the recent development of immersive technologies, virtual reality (VR), augmented reality (AR), and mixed reality (MR) have the potential to offer more comprehensive and in-depth 3D visualization in which the user is fully immersed in the digital brain. In [1], Morales Mojica implemented an AR interface that enables the visualization of the complex brain vasculature and anatomical structures derived from MRI data for the planning of neurosurgical procedures. Similarly, Chen [2] explored the application of VR technology to visualize the human brain from high-resolution images of functional MRI. The technologies have also a lot of applications in the education and medical fields [3]–[7]. Combined with AR and VR techniques, MR technique creates an interactive environment where physical and digital objects coexist, which enables users to interact with the digital objects overlaid in the physical world. More specifically, one can walk around, grab, rotate, scale, and move virtual objects using gestures or controllers, creating a sense of presence and realism. Another important feature of MR is remote collaboration that allows users located in different places to share a virtual space and collaborate in real-time.

Recently, MR has received a lot of attention due to its powerful capabilities for interactive 3D visualization [8]–[12]. An MR application based on the building information modeling was developed to enhance the management of bridge inspection and maintenance tasks remotely from the office [13]. Leuze [14] provided guidance for brain stimulation treatment of depression using an MR device to project the

The research is supported by FDCT 0141/2020/A3, 0084/2023/ITP2. F. Qi is the first author and X.-C. Cai is the corresponding author of the paper. Email: xccai@um.edu.mo

979-8-3315-1599-7/24/$31.00 ©2024 IEEE
DOI 10.1109/MetaCom62920.2024.00018

individual MRI data onto the subject's head so that the operator can view the brain anatomy directly. Petersen [15] designed an MR holographic interface to build human axonal pathways models by integrating the human histological and structural MRI data.

Computational fluid dynamics (CFD) is a classical technique to numerically simulate and predict the behavior of fluid flows. More recently, researchers use CFD-based methods to study the behavior of blood flows in, for examples, abdominal aorta [16], pulmonary artery [17], hepatic artery and vein [18], coronary artery [19], cerebral artery [20]–[22] and cardiovascular system [23]. In this paper, we are particularly interested in cerebral aneurysms, for which studies have indicated that the hemodynamic factors [24] such as wall shear stress (WSS) [25] and flow patterns [26] are strongly correlated to the risk of rupture. Unlike 2D medical images, these CFD results are all 3D, and when viewed in VR devices, they provide more realism than viewed on traditional 2D computer monitors. For example, Shi [27] developed a software platform to modify the vascular geometry and visualize the simulation result of blood flows using a VR interface. Baheri Islami [28] introduced a VR visualization of the CFD-based simulation of blood flows in an aneurysmal cerebral artery treated with flow diverter stents. Zhu [29] proposed an MR system to show the arterial network interactively as well as the distribution of the blood flow using a reduced 1D artery-network model. Gong [30] built an MR interactive platform to visualize the physical motion and deformation of a digital human heart in real time by numerically solving 3D nonlinear elasticity equations on a parallel computer. These interactive platforms have many potential applications in the medical field for the training of physicians, for remote collaborations, and for the planning of complicated surgery.

In this paper, we extend the interactive platform introduced in [30] for a digital human brain, and the main purposes are the intuitive visualization of the digital brain and the interactive hemodynamic computation of the cerebral artery with aneurysms. The current version of our digital brain consists of the anatomical structures including the gray and white matters as well as the major cerebral artery network. Each structure can be observed immersively and individually by transparentizing the other components. For the brain tissue, we attach the functional atlas and provide the hand gesture operation to isolate certain functional areas such as cognition, memory, and language, etc. The functional areas of the matters and the atlas are mapped onto each other. When the index finger touches an area, the corresponding color, function, and their values of the area, volume and thickness are viewable in the holographic glasses.

The other important purpose of the proposed platform is for the planning of cerebral aneurysm surgery. Through the connection of the platform with a parallel computer, we can numerically simulate the behavior of the blood flow using CFD-based methods and observe the distributions of pressure, velocity, streamline and wall shear stress for different surgical plans before the actual surgery is performed. Zooming in on the aneurysmal region, the local hemodynamic features can be viewed directly, which offers a lot of insight into the risk of rupture. The platform provides a few virtual operations through hand gestures, such as a typical operation to clip off the aneurysm, and then visualize the corresponding post-surgery behavior of the blood flow. This functionality gives the surgeons several options to compare and analyze the hemodynamic differences before and after the surgery. The platform plays an important role to integrate MR and CFD and also allows the real time control of the physicians.

The rest of the paper is organized as follows. In Section 2, we present a mixed reality platform for the visualization of the human brain based on a holographic device, and also for the interactive computation of blood flows in the cerebral artery. In Section 3, we show some functionalities of the platform to evaluate some suggested surgical plans that may change the behavior of the blood flow before and after the possible operation. Some conclusions are given in Section 4.

II. Mixed reality visualization and interactive computation of the human brain

In this section, we describe the details of a platform for the visualization of some structures and functional areas of a digital brain, as well as the interactive hemodynamic computation in the cerebral artery. 3D geometries of the patient-specific brain tissue and cerebral artery are obtained from the segmentation of high-resolution MRI images as shown in Fig. 1. In Fig. 2, we present the major components of the proposed mixed reality platform: (a) A digital brain consisting of the gray and white matters, and the cerebral artery; (b) The digital brain tissues and labeled functional areas; (c) Patient-specific arteries with highlighted aneurysms; (d) A pair of holographic glasses with multiple cameras to track the user's hand movements and gestures and the device is pre-loaded with the digital brain; (e) A GPU server serving as the platform manager (PM) that is wirelessly connected to the glasses and also connected to (f) A parallel computer that carries out hemodynamic computation in near real-time.

A. Interactive holographic device

In this subsection, we give an overview of the holographic device in which the head skin and a digital brain with the gray matter, the white matter, and the cerebral artery are pre-loaded. The device consists of a pair of MR-based glasses equipped with cameras that are capable of capturing and recognizing the user's hand movements and gestures within the cameras' field of view in real-time. When wearing the glasses, one can see the surrounding physical objects and the digital brain which can be moved to overlap with the real object. Thanks to the ability to track the position and movement of the user's head, the visualization is adjusted automatically according to the user's location and viewpoint. Based on the built-in interactive functions, one is able to move, rotate and zoom-in or -out of the brain as well as other virtual objects. Moreover, for observing the precise spatial relationships among structures in depth and enabling personalized interactions with these structures, the

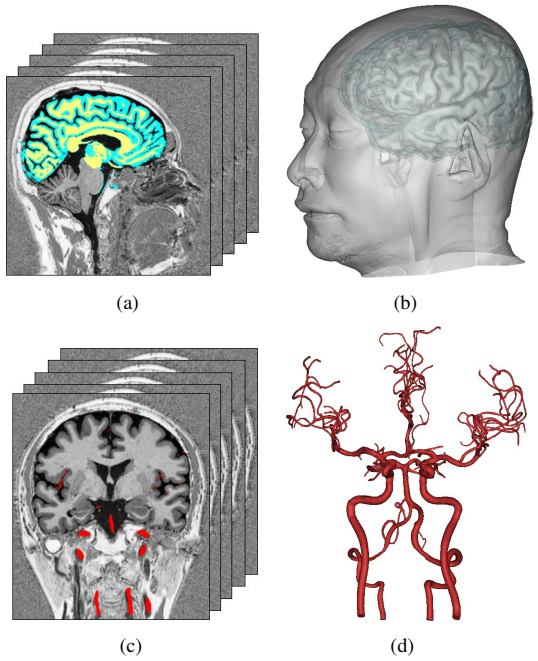

Fig. 1. (a) Raw 2D MRI images of the brain tissues marked in blue and yellow, respectively, (b) reconstructed 3D brain tissues, (c) raw 2D MRI images of the cerebral artery marked in red, (d) reconstructed 3D cerebral artery.

platform provides various user-defined functions. For example, by adjusting the sliders we implemented in the platform, the user can easily regulate the level of transparency of the objects. With a press of the button, the user can selectively reveal or conceal specific brain structures as desired. Additionally, a transparent box is employed to slice through the digital brain, generating cross-sectional views of the region of interest and enabling examination of internal structures from various angles and depths. For the gray and white matter, by touching any area of interest, the corresponding functional area can be highlighted using a color from the brain atlas. Furthermore, the numerical values of the area, volume and thickness of the touched area are also displayed on top of the matters, providing additional information to the user.

To help the diagnosis and surgery planning related to cerebral aneurysm, a user-friendly menu is implemented, as an example, the virtual clipping surgery, allowing for the selection of various procedure. For instance, by tapping on the 'Neck plane' button, a virtual clipping plane is activated, and it can be repositioned to the right location and with the right level of transparency (as shown in Fig. 3). This application provides surgeons with the means to enhance their understanding and plan the optimal position and angle for precise clip placement.

B. Patient-specific hemodynamics and computations in the cerebral artery

Numerical simulation is an important tool for studying the blood flow in the cerebral artery, especially for the comparison of the flow patterns before and after a certain surgery. In the hemodynamic analysis, a set of partial differential equations is solved based on physical laws such as the conservation of momentum and mass. In this paper, we consider the unsteady incompressible Navier-Stokes equations whose variables are the blood velocity $\boldsymbol{u}$ and pressure p, and the values of the blood density ρ and dynamic viscosity μ are assumed to be given. To ensure the uniqueness and existence of the solution of this model, suitable initial and boundary conditions are prescribed. For the initial condition, we simply assume the velocity is zero. For the boundary conditions, on the inlet and wall, we apply the individual pulsating velocity and no-slip velocity Dirichlet boundary conditions, respectively; on the outlets, the resistance boundary condition is employed with constant resistance determined by Murray's law. The computational domain and blood pressure data are patient-specific. To discretize the Navier-Stokes equations, we use a stabilized finite element method in space and a second-order backward differentiation formula in time.

In the numerical computation, we focus on two important issues, namely the wall shear stress (WSS) [25] and the flow pattern [26] since they are highly correlated to the risk of rupture. WSS describes the shear force on the wall of the aneurysm, and it can be computed by

$$WSS = \mu|\nabla \boldsymbol{u} \cdot \boldsymbol{n} - ((\nabla \boldsymbol{u} \cdot \boldsymbol{n}) \cdot \boldsymbol{n})\boldsymbol{n}|, \qquad \text{(II.1)}$$

where $\boldsymbol{n}$ is the outward unit normal vector of the wall. It is affected by the velocity, the viscosity and the characteristics of the surface of the wall. Both high and low values of WSS may degenerate the aneurysm wall and trigger the rupture. Flow patterns are the structure and characteristics of vortices in the aneurysm. We often claim that the flow patterns are complex if there are more than one vortex and/or if the flows are unstable in the sense that the vortex structures change significantly in a short period of time. The complexity and stability of vortices are important indicators when we try to predict the risk of rupture. In order to quantify the flow patterns, the normalized helicity and vortex cores are considered. The normalized helicity [31] is defined as

$$H_n = \frac{\boldsymbol{w} \cdot \boldsymbol{u}}{|\boldsymbol{w}||\boldsymbol{u}|}, \qquad \text{(II.2)}$$

where $\boldsymbol{w} = \text{curl } \boldsymbol{u}$ is the vorticity. The sign of H_n is used to distinguish the primary (positive) and secondary (negative) vortices. Primary refers to vortices generated directly by the fluid flow and secondary are these from the interaction between primary vortices. We use this value to reflect the complexity of the flow patterns. The vortex cores are the central lines of the vortex around which the blood flows rotate and can be detected using the eigenvector method. We define the Jacobian matrix of the velocity vector at a given point $\boldsymbol{u}$ as $J = \nabla \boldsymbol{u}$, which is a three-by-three matrix. The vortex occurs when the Jacobian matrix has one real and a pair of complex-conjugate eigenvalues, which implies that

$$P := \left(\frac{Q_J}{3}\right)^3 + \left(\frac{R_J}{2}\right)^2 > 0,$$

where $Q_J = -1/2\text{tr}(J^2)$, $R_J = -\det(J)$, and here the incompressibility condition is used. Then the vortex cores can

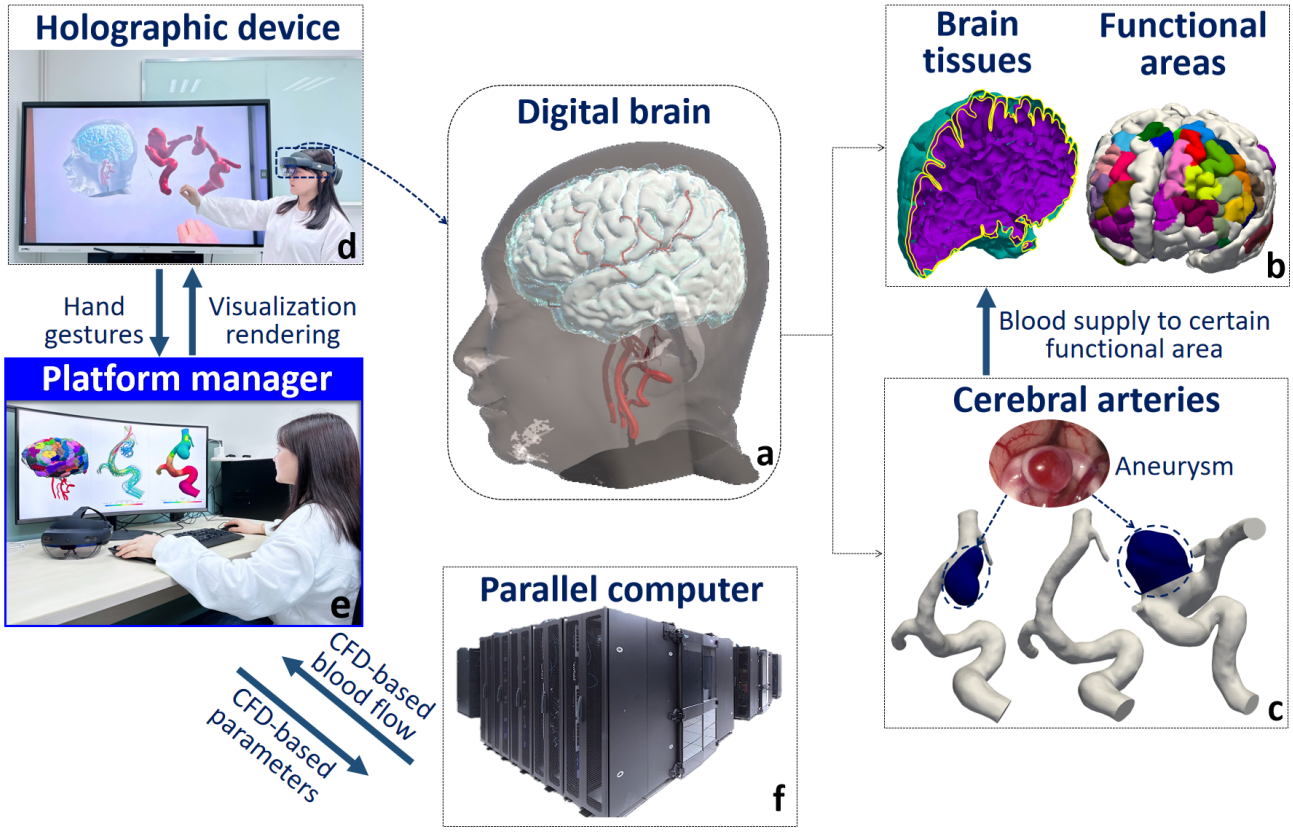

Fig. 2. The basic components of the proposed platform. (a) a digital brain including the gray and white matters, and the cerebral artery; (b) individual components of the digital brain; (c) portions of the artery with aneurysms; (d) a pair of glasses and multiple cameras; (e) a GPU workstation serving as the platform manager responsible for receiving the command from the holographic device, controlling the computation on the parallel computer and visualizing the computational results; (f) a parallel computer to perform large-scale hemodynamic calculations.

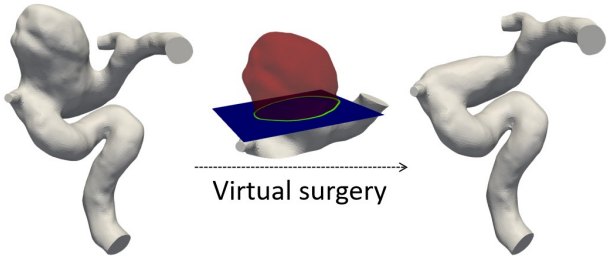

Fig. 3. In the current implementation, the aneurysm-removing process is modeled by the cut of the aneurysm by a plane.

be defined as a collection of points in the following set [32], i.e.,

$$V_c = \{x \in \Omega_a | P(x) > 0, \boldsymbol{u} - (\boldsymbol{u} \cdot \boldsymbol{e})\boldsymbol{e} = 0, \},$$

or the equivalent parallel vector method [33]

$$V_c = \{x \in \Omega_a | P(x) > 0, J\boldsymbol{u} \parallel \boldsymbol{u}, J = \nabla \boldsymbol{u}\}, \qquad \text{(II.3)}$$

where $\boldsymbol{e}$ is the eigenvector corresponding to the real eigenvalue, Ω_a is the aneurysm part of the artery.

C. Nonlinear solver and aneurysm risk assessment process

To solve the large, sparse nonlinear systems of algebraic equations from the finite element discretization on parallel computers, we partition the arterial mesh into np subdomains (See Fig. 4 for an example) and adopt an inexact Newton method for the nonlinear system and a Krylov subspace method for the linearized Jacobian system with the additive Schwarz preconditioner, i.e., the Newton-Krylov-Schwarz (NKS) method; see Fig. 5. Based on the numerical simulation for a complete cardiac cycle, we can evaluate the risk of the rupture of the cerebral aneurysm by the indexes introduced above. The process of the risk assessment is shown in Fig. 6. We first extract the numerical velocity and pressure values in the aneurysm region Ω_a, and then compute these indexes and see if any of them are over the given thresholds, indicating a surgery is necessary.

We run the MR-based virtual surgery and the corresponding CFD-based simulations repeatedly to help find the suitable treatment plan for the actual surgery. In the process of virtual surgeries, we can try different shapes of clips, different locations or different types of surgery.

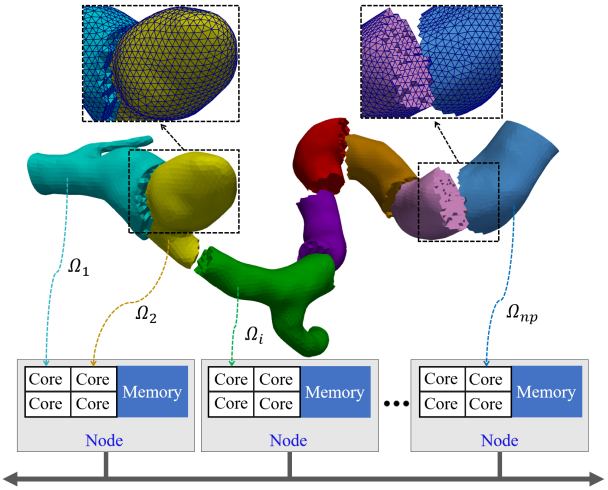

Fig. 4. A sample partition of the global mesh into 8 subdomains highlighted by different colors. Subproblems associated with subdomains are run on different cores of the parallel computer.

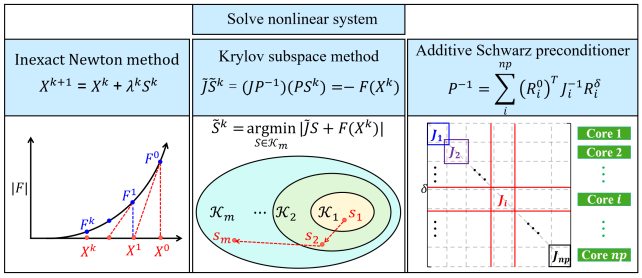

Fig. 5. Newton-Krylov-Schwarz method for solving the nonlinear discretized system of the blood flow problem. (1) Inexact Newton method employs a linearization technique to iteratively solve the nonlinear system; (2) the Krylov subspace method is used to find the approximate solution of the linearized system in Krylov subspaces; (3) the additive Schwarz preconditioner is introduced to accelerate the Krylov subspace iteration in parallel.

III. Some Early Experiences and Discussions

In this section, we focus on two applications of the proposed platform and use some patient-specific data as examples to demonstrate the functions and operations of the platform. The first application is to visualize the human brain through hand gestures from both the built-in functions provided by the MRTK3 package and our user-defined functions. The second application aims at assessing the surgery of cerebral aneurysms based on an interactive computational simulation of the blood flows.

A. Mixed reality visualization of the human brain

The visualization in the holographic device is realized by a two step process, first we render the objects on the GPU-based PM, then using the remoting function we stream the content to the holographic device in real time. Through the built-in hand gestures, the user can traverse through and peel away layers of the digital brain to reveal some of the underlying structures such as the gray matter, white matter and cerebral artery. In the

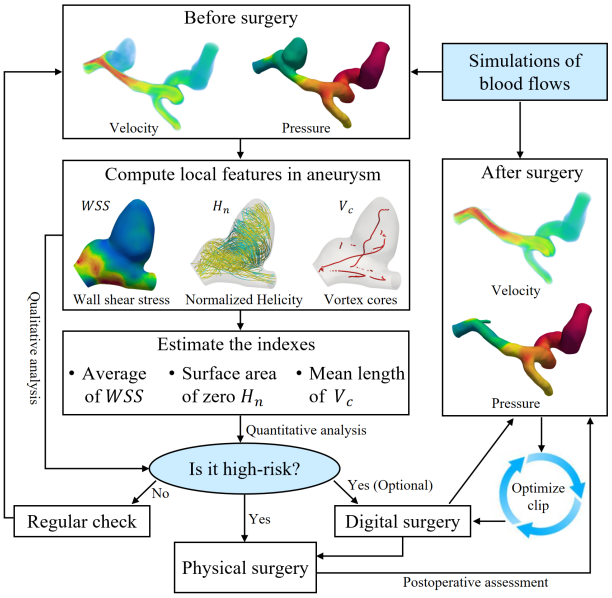

Fig. 6. The process diagram of the assessment of the aneurysmal risk and the surgical planning based on the proposed platform.

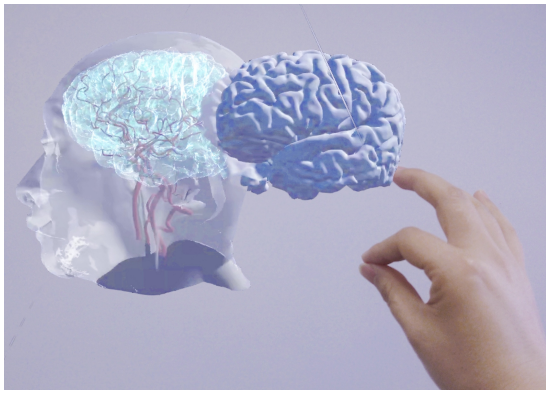

Fig. 7. An operation of dragging the white matter out from the digital brain through a pinch of the right thumb and the index finger. The skin and the gray matter are made fully transparent by two sliders.

virtual space, these structures are individual objects and can be dragged, zoomed in or out and viewed along the surrounding objects with different perspectives. In Fig. 7, the white matter is taken out by a pinch of the right thumb and the index finger. Note that some sliders are also designed to adjust the level of transparency of the structures. As an example, we make the skin and gray matter fully transparent to observe the spatial position of the white matter by sliding the corresponding two sliders. This enables us to view every detail and the precise spatial relationship among structures.

To understand the functionalities of the brain, the gray and white matters are usually divided into functional areas. In general, a function such as the memory function relies on multiple areas interacting with each other. In the platform, we use the human Brainnetome atlas [34] with 210 distinct

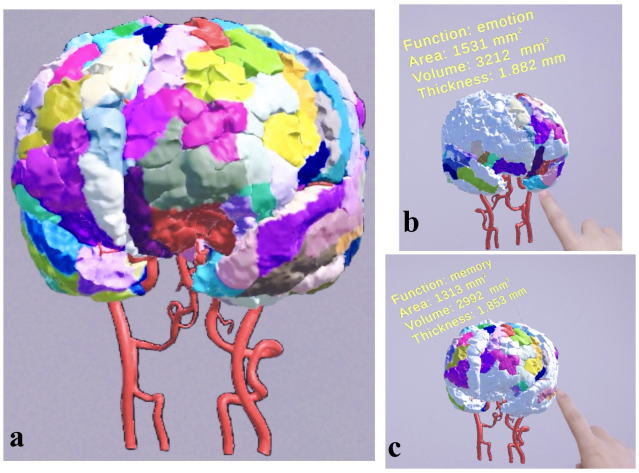

Fig. 8. (a) Initial default state with all highlighted functional areas; (b) and (c) activated areas matching the emotion and the memory functions, respectively, as well as the structural information of the area, the volume and the thickness by touching the corresponding area with the right index finger.

subdivisions and define some hand gestures and operations to control the visualization of functional areas, specifically including

- The initial state: all functional areas of the brain are highlighted by different colors; see the left subfigure of Fig. 8.
- To activate a functional area: when the user touches any area of interests with the right index finger, the areas whose functions match the function of the touched area are activated and highlighted with colors, and the other areas become white. For examples, in the right subfigures of Fig. 8, the emotion and the memory functions are, respectively, highlighted as both areas are finger touched. At the same time, the structural information associated with these areas including the values of the area, the volume and the thickness are displayed near the areas.
- The activated areas remain activated until the user touches another functional area, and the user can move around and view different areas.
- The 'Restore' button allows the user to return to the initial state.

These functions of the platform can help users immersively view the areas of interest and find the basic properties of the areas. Moreover, it is possible to use the platform to compare the individual differences in the functional areas of different patients, facilitating certain studies of the brains.

B. Interactive computation and assessment of blood flows in aneurysmal cerebral arteries

The proposed platform also provides an opportunity to dynamically visualize the results from the numerical computation of the blood flows when the user chooses to interactively modify the arterial geometry or model parameters by hand gestures. With this function, the user sees clearly the correlation between the geometry or parameters changes and the resulting changes of the blood flows. In this subsection, we demonstrate an application of the platform in the computation and visualization of blood flows in the cerebral artery with aneurysm. More specifically, we consider (1) the virtual clipping operation for cerebral aneurysms; (2) the hemodynamic computation and visualization of numerical results; (3) the visualization of local hemodynamic features in aneurysms and risk assessment.

As an example, in the platform, we introduce a virtual menu for cerebral aneurysms with buttons labeled with 'Aneurysm', 'Neck plane' and 'Surgical clip' that are used to navigate different stages during the surgical planning procedure, as shown in Fig. 9. First, we press the 'Aneurysm' button to detect and highlight the aneurysm region. Then, by clicking the 'Neck plane', a neck plane emerges and can be moved towards the aneurysm, and its size, position, and angle can all be adjusted. The aneurysm can be virtually removed to obtain an artery if we click on the 'Surgical clip' button, which in a way suggests that the surgery is complete. Note that the location information of the plane in the clipping step is automatically sent to the PM, and the PM then sends back the modified artery to the holographic glasses for visualization. Furthermore, we also provide options to reposition the neck plane in case of any operational error or when the desired requirements are not satisfied. The virtual surgical application not only provides a way to train new users of the procedure but also predicts some hidden risks in the planned surgery.

After the user performs the virtual surgery, both the original and the repaired arteries appear in the virtual space. By clicking the 'Compute' button we activate the computation process for the selected geometry. For example, the user can first select the pre-operative artery, then trigger the 'Compute' button, and the PM will generate a mesh and send the mesh data to the parallel computer for the numerical computation. After the calculation, all the results are sent to the PM who then delivers them to the holographic glasses, in which some computed field such as the pressure appears near the corresponding artery by default. The velocity streamlines and WSS can also be viewed by bringing up the menu and clicking the specified buttons, as shown in Fig. 10. Note that the same operations can be carried out for the repaired artery. In addition, to view the value of these numerical results at any point on the arterial wall, we create a 'touch' gesture for the index finger, see Fig. 10. The visualization of both pre- and post-operative hemodynamic results within the same virtual space provides valuable support to surgeons for comparing and analyzing the differences.

Local hemodynamic features in the aneurysm are very important to assess the risk of rupture. Benefiting from the MR technique in the platform, the local features like pressure and WSS can be visualized directly using the hand gesture to locate and zoom in on the aneurysm. To see other local features such as the velocity streamlines, the helicity and the vortex cores, we first compute them on the PM since the computations are considered too expensive on the holographic device, and then we send the requested information wirelessly to the holographic glasses. Based on the local features, the

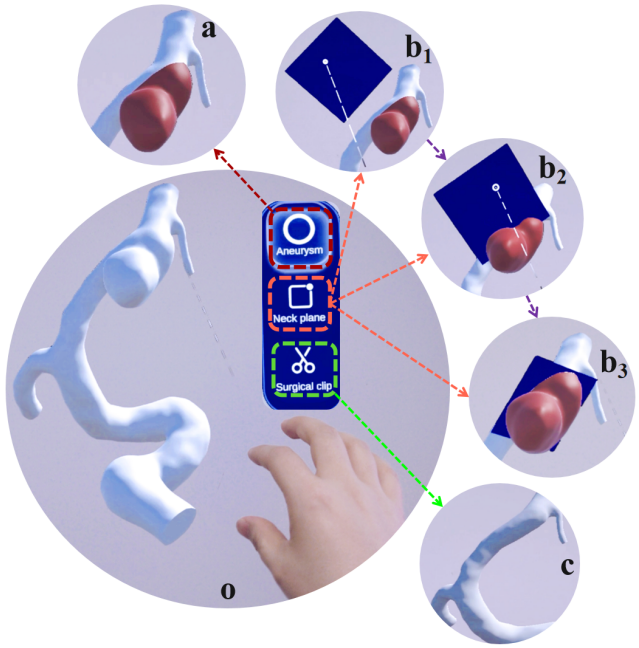

Fig. 9. Procedure for a virtual surgery: (o) the interactive menu for a patient-specific cerebral aneurysm with three buttons acting on the aneurysm, the neck plane and the surgical clip, respectively, where the corresponding action can be triggered by a 'click' operation; (a) the aneurysm located and highlighted in red by the 'Aneurysm' button; (b) a plane used as the virtual surgical tool activated by the 'Neck plane' button, where it presents three different states during surgery: appearance near the aneurysm by default (b_1), spatial adjustment through moving and scaling (b_2), the final placement with a suitable size, position and angle (b_3); (c) an artery without aneurysm by pressing 'Surgical clip'.

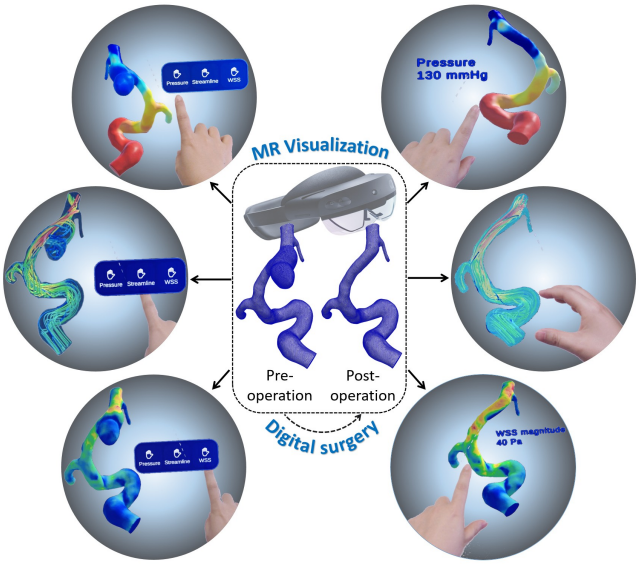

Fig. 10. Holographic-based hemodynamic visualization for the same patient before and after a surgery. The distributions of the blood pressure, the velocity streamlines and WSS can be viewed together or separately by clicking the specified button on the virtual screen. The value at this point is displayed when touching a certain point with the index finger.

risk of rupture can sometimes be evaluated qualitatively and quantitatively. For instance, complex vortex cores are often more risky than simple vortex cores. Moreover, the risk level can also be assessed based on the mean and the oscillatory index of WSS, the surface area of zero helicity and the average length of vortex cores, see Table I, in which we list three cases and show these local features as well as the corresponding indexes. Note that the local features and the indexes are strongly correlated to the rupture for these cases.

TABLE I

LOCAL HEMODYNAMIC FEATURES, INDEXES AND RISK STATUSES FOR THREE DIFFERENT CASES. (1) INDEX OF WSS (PA): THE MEAN WSS; (2) INDEX OF HELICITY (CM^2): THE SURFACE AREA OF ZERO HELICITY; (3) INDEX OF VORTEX CORES (CM): THE AVERAGE LENGTH OF VORTEX CORES.

Case	WSS	Helicity	Vortex cores	Status
C01	Index: 8.63	Index: 2.52	Index: 2.07	Rupture
C02	Index: 5.84	Index: 8.55	Index: 3.05	Rupture
C03	Index: 2.62	Index: 1.07	Index: 0.64	Unrupture

IV. SOME CONCLUDING REMARKS

In this paper, we developed an immersive and interactive platform for the visualization and the computation of the hemodynamics of a digital brain based on the MR technique and a connected parallel computer. The current version of the digital brain consists of the white and gray matters, and the cerebral artery. The platform provides a suite of gesture controlled functions related with cerebral aneurysm including the CFD-based simulation of blood flows, hemodynamic-based risk assessments of rupture, some simulated surgical options, and the comparison of the blood flow dynamics before and after surgery. The system is implemented with a GPU-based platform manager that is wirelessly connected with a pair of holographic device and directly connected a parallel computer. Viewing from the holographic device, the structures and functional areas of the brain are easy to visualize separately through hand gestures and the spatial relationship between structures becomes more obvious. The platform has many potential applications in, for examples, reducing the risk of neurosurgeries by offering more comprehensive surgical planning, improving precision, and enabling preoperative

practice. The visualization of functional areas may help relate the cerebral arteries to their downstream functional areas, and also decrease the damage to functional areas in interventional operations.

REFERENCES

[1] C. M. Morales Mojica, J. D. Velazco-Garcia, E. P. Pappas, T. A. Birbilis, A. Becker, E. L. Leiss, A. Webb, I. Seimenis, and N. V. Tsekos, "A holographic augmented reality interface for visualizing of MRI data and planning of neurosurgical procedures," *Journal of Digital Imaging*, vol. 34, pp. 1014–1025, 2021.

[2] B. Chen, J. Moreland, and J. Zhang, "Human brain functional MRI and DTI visualization with virtual reality," in *World Conference on Innovative Virtual Reality*, vol. 44328, 2011, pp. 343–349.

[3] S. Zafar and J. J. Zachar, "Evaluation of HoloHuman augmented reality application as a novel educational tool in dentistry," *European Journal of Dental Education*, vol. 24, no. 2, pp. 259–265, 2020.

[4] A. W. K. Yeung, A. Tosevska, E. Klager, F. Eibensteiner, D. Laxar, J. Stoyanov, M. Glisic, S. Zeiner, S. T. Kulnik, R. Crutzen *et al.*, "Virtual and augmented reality applications in medicine: analysis of the scientific literature," *Journal of Medical Internet Research*, vol. 23, no. 2, p. e25499, 2021.

[5] C. Jung, G. Wolff, B. Wernly, R. R. Bruno, M. Franz, P. C. Schulze, J. N. A. Silva, J. R. Silva, D. L. Bhatt, and M. Kelm, "Virtual and augmented reality in cardiovascular care: state-of-the-art and future perspectives," *Cardiovascular Imaging*, vol. 15, no. 3, pp. 519–532, 2022.

[6] M. Venkatesan, H. Mohan, J. R. Ryan, C. M. Schürch, G. P. Nolan, D. H. Frakes, and A. F. Coskun, "Virtual and augmented reality for biomedical applications," *Cell Reports Medicine*, vol. 2, no. 7, 2021.

[7] V. Chheang, D. Schott, P. Saalfeld, L. Vradelis, T. Huber, F. Huettl, H. Lang, B. Preim, and C. Hansen, "Advanced liver surgery training in collaborative VR environments," *Computers & Graphics*, 2024.

[8] J. Cartucho, D. Shapira, H. Ashrafian, and S. Giannarou, "Multimodal mixed reality visualisation for intraoperative surgical guidance," *International Journal of Computer Assisted Radiology and Surgery*, vol. 15, pp. 819–826, 2020.

[9] N. Xiang, H.-N. Liang, L. Yu, X. Yang, and J. J. Zhang, "A mixed reality framework for microsurgery simulation with visual-tactile perception," *The Visual Computer*, vol. 39, no. 8, pp. 3661–3673, 2023.

[10] E. Colombo, B. Lutters, T. Kos, and T. Van Doormaal, "Application of virtual and mixed reality for 3D visualization in intracranial aneurysm surgery planning: A systematic review," *Frontiers in Surgery*, vol. 10, 2023.

[11] J. L. McJunkin, P. Jiramongkolchai, W. Chung, M. Southworth, N. Durakovic, C. A. Buchman, and J. R. Silva, "Development of a mixed reality platform for lateral skull base anatomy," *Otology & Neurotology*, vol. 39, no. 10, pp. e1137–e1142, 2018.

[12] J. Wang, Y. Zhao, X. Xu, Q. Wang, F. Li, S. Zhang, Z. Gan, R. Xiong, J. Zhang, and X. Chen, "A patient-specific, interactive, multiuser, online mixed-reality neurosurgical training and planning system," *Neurosurgical Focus*, vol. 56, no. 1, p. E15, 2024.

[13] D.-C. Nguyen, T.-Q. Nguyen, R. Jin, C.-H. Jeon, and C.-S. Shim, "Bim-based mixed-reality application for bridge inspection and maintenance," *Construction Innovation*, vol. 22, no. 3, pp. 487–503, 2022.

[14] C. Leuze, G. Yang, B. Hargreaves, B. Daniel, and J. A. McNab, "Mixed-reality guidance for brain stimulation treatment of depression," in *2018 IEEE International Symposium on Mixed and Augmented Reality Adjunct (ISMAR-Adjunct)*. IEEE, 2018, pp. 377–380.

[15] M. V. Petersen, J. Mlakar, S. N. Haber, M. Parent, Y. Smith, P. L. Strick, M. A. Griswold, and C. C. McIntyre, "Holographic reconstruction of axonal pathways in the human brain," *Neuron*, vol. 104, no. 6, pp. 1056–1064, 2019.

[16] S. Qin, R. Chen, B. Wu, W.-S. Shiu, and X.-C. Cai, "Numerical simulation of blood flows in patient-specific abdominal aorta with primary organs," *Biomechanics and Modeling in Mechanobiology*, vol. 20, pp. 909–924, 2021.

[17] F. Kong, V. Kheyfets, E. Finol, and X.-C. Cai, "An efficient parallel simulation of unsteady blood flows in patient-specific pulmonary artery," *International Journal for Numerical Methods in Biomedical Engineering*, vol. 34, no. 4, p. e2952, 2018.

[18] Z. Lin, R. Chen, B. Gao, S. Qin, B. Wu, J. Liu, and X.-C. Cai, "A highly parallel simulation of patient-specific hepatic flows," *International Journal for Numerical Methods in Biomedical Engineering*, vol. 37, no. 6, p. e3451, 2021.

[19] Z. Yan, Z. Yao, W. Guo, D. Shang, R. Chen, J. Liu, X.-C. Cai, and J. Ge, "Impact of pressure wire on fractional flow reserve and hemodynamics of the coronary arteries: A computational and clinical study," *IEEE Transactions on Biomedical Engineering*, vol. 70, no. 5, pp. 1683–1691, 2022.

[20] R. Chen, B. Wu, Z. Cheng, W.-S. Shiu, J. Liu, L. Liu, Y. Wang, X. Wang, and X.-C. Cai, "A parallel non-nested two-level domain decomposition method for simulating blood flows in cerebral artery of stroke patient," *International Journal for Numerical Methods in Biomedical Engineering*, vol. 36, no. 11, p. e3392, 2020.

[21] Y. Liu, F. Qi, and X.-C. Cai, "An aneurysm-specific preconditioning technique for the acceleration of Newton-Krylov method with application in the simulation of blood flows," *International Journal for Numerical Methods in Biomedical Engineering*, vol. 39, no. 12, p. e3771, 2023.

[22] J. Xie, Z. Cheng, L. Gu, B. Wu, G. Zhang, W. Shiu, R. Chen, Z. Wang, C. Liu, J. Tu *et al.*, "Evaluation of cerebrovascular hemodynamics in vascular dementia patients with a new individual computational fluid dynamics algorithm," *Computer Methods and Programs in Biomedicine*, vol. 213, p. 106497, 2022.

[23] A. Quarteroni, A. Manzoni, and C. Vergara, "The cardiovascular system: mathematical modelling, numerical algorithms and clinical applications," *Acta Numerica*, vol. 26, pp. 365–590, 2017.

[24] D. M. Sforza, C. M. Putman, and J. R. Cebral, "Hemodynamics of cerebral aneurysms," *Annual Review of Fluid Mechanics*, vol. 41, pp. 91–107, 2009.

[25] M. Shojima, M. Oshima, K. Takagi, R. Torii, M. Hayakawa, K. Katada, A. Morita, and T. Kirino, "Magnitude and role of wall shear stress on cerebral aneurysm: computational fluid dynamic study of 20 middle cerebral artery aneurysms," *Stroke*, vol. 35, no. 11, pp. 2500–2505, 2004.

[26] J. R. Cebral, M. A. Castro, J. E. Burgess, R. S. Pergolizzi, M. J. Sheridan, and C. M. Putman, "Characterization of cerebral aneurysms for assessing risk of rupture by using patient-specific computational hemodynamics models," *American Journal of Neuroradiology*, vol. 26, no. 10, pp. 2550–2559, 2005.

[27] H. Shi, J. Ames, and A. Randles, "Harvis: an interactive virtual reality tool for hemodynamic modification and simulation," *Journal of Computational Science*, vol. 43, p. 101091, 2020.

[28] S. Baheri Islami, M. Wesolowski, W. Revell, and X. Chen, "Virtual reality visualization of CFD simulated blood flow in cerebral aneurysms treated with flow diverter stents," *Applied Sciences*, vol. 11, no. 17, p. 8082, 2021.

[29] L. Zhu, D. Chen, Y. Du, J. Yin, W. Xia, and Y. J. Zhang, "Vasnet_mr: interactive exploration of vascular network blood flow distribution with mixed reality," *Available at SSRN 4175927*.

[30] Y. Gong, F. Qi, J.-Y. Wang, Y. Liu, T. Ma, Z. Cheng, Y. Jiang, R. Chen, X. Wang, L. Luo *et al.*, "An interactive platform for a high performance digital twin of a human heart," in *2023 IEEE International Conference on Metaverse Computing, Networking and Applications (MetaCom)*. IEEE, 2023, pp. 193–200.

[31] Y. Levy, D. Degani, and A. Seginer, "Graphical visualization of vortical flows by means of helicity," *AIAA J.*, vol. 28, no. 8, pp. 1347–1352, 1990.

[32] D. Sujudi and R. Haimes, "Identification of swirling flow in 3-D vector fields," in *12th Computational Fluid Dynamics Conference*, 1995, p. 1715.

[33] M. Roth and R. Peikert, "A higher-order method for finding vortex core lines," in *Proceedings Visualization'98 (Cat. No. 98CB36276)*. IEEE, 1998, pp. 143–150.

[34] L. Fan, H. Li, J. Zhuo, Y. Zhang, J. Wang, L. Chen, Z. Yang, C. Chu, S. Xie, A. R. Laird *et al.*, "The human brainnetome atlas: a new brain atlas based on connectional architecture," *Cerebral Cortex*, vol. 26, no. 8, pp. 3508–3526, 2016.